DNA DAMAGE IN SYNCHRONIZED HELA CELLS IRRADIATED WITH ULTRAVIOLET

C. S. DOWNES, A. R. S. COLLINS, AND R. T. JOHNSON, *Department of Zoology, University of Cambridge, CB2 3EJ, England*

ABSTRACT The lethal effect of UV radiation on HeLa cells is least in mitosis and greatest in late G_1–early S. Photochemical damage to HeLa DNA, as measured by thymine-containing dimer formation and by alkaline sucrose sedimentation, also increases from mitosis towards early S phase. Computer simulations of UV absorption by an idealized HeLa cell at different stages of the cell cycle indicate that changes in damage could be due solely to changes in chromatin geometry. But survival is not exclusively a function of damage.

INTRODUCTION

Cell killing by ultraviolet radiation (UV) is unlikely to be simply related to the amount of UV reaching the cell surface, for at least two reasons. First, the dose of UV reaching the DNA (probably the most significant target for UV at 254 nm) will be less than the UV incident on the whole cell, because of absorption and scattering at the cell surface and within the cell. Second, whether the cell survives UV damage will depend on its capacity for repair.

These factors influencing survival are likely to vary between different cell types and within a single cell type during traverse of the cell cycle. In this paper, we attempt to relate variations in survival of HeLa cells irradiated at different points in the cell cycle to variations in the proportion of the incident radiation that reaches the DNA. The effect of UV on the DNA has been assessed by measuring the efficiency of cyclobutane pyrimidine dimer production and by examining the sedimentation behavior of irradiated DNA on alkaline sucrose gradients modified to display possible conformational changes. The results are discussed in the light of a model that attempts to explain UV sensitivity as a function of target geometry.

MATERIALS AND METHODS

Cell Culture and Synchronization Procedure

HeLa cells were routinely cultured in suspension in spinner flasks, in Eagle's minimal essential medium supplemented with 5% fetal calf serum and nonessential amino acids. When isotopically labeled material was required, cells were transferred to 150 mm or 60 mm plastic Petri dishes (Falcon Plastics, BioQuest, Oxnard, Calif., or A/S Nunc, Kamstrup, DK-4000 Roskilde, Denmark) and labeled with [^{3}H]thymidine (Radiochemical Centre, Amersham, England) at 0.04 μCi/ml (sp act 20 Ci/mmol) for 1 d in the thymine dimer studies, or at 0.04 μCi/ml (sp act 2 Ci/mmol) for 6 h in the alkaline sucrose experiments. Labeling was carried out before synchronization.

Mitotic cells, with a synchrony of 95% or more, were obtained by a thymidine block (2.5 mM, 20–24 h) followed, after a 4-h interval, by a 9-h block with high-pressure nitrous oxide (1). If not used at once, the cells were allowed to pass into interphase in suspension culture (survival experiments and dimer analyses) or in Petri dishes (alkaline sucrose studies). The start of G_1 phase

occurred approximately 2 h after release from the nitrous oxide block. Progress through the cell cycle is expressed (in figures, etc.) as the time in hours from this point.

In one experiment, xeroderma pigmentosum cells, kindly supplied by Dr. Karl Sperling of the Free University of Berlin, were used. They were cultured as described previously (2).

UV Irradiation

Cells were irradiated with a Philips germicidal lamp (Philips Electrical Ltd., Sywell, Northampton, England), emitting predominantly at 254 nm; for dimer analyses and alkaline sucrose sedimentation studies, at a rate of 3·3 $Jm^{-2}s^{-1}$ measured at the position of the cells with a model IL500 research radiometer (International Light, Inc., Newburyport, Mass.), and for survival experiments, at 0·1 or 1·0 $Jm^{-2}s^{-1}$. For survival experiments and dimer analyses, cells were irradiated at a density of 10^5/ml in 150-mm dishes in 5 ml of growth medium, including 5% fetal calf serum, or of phosphate-buffered saline (PBS) (3). For alkaline sucrose sedimentation studies, the cell density was 1.3×10^5/ml and 1.5 ml of cells in medium were irradiated in 60 mm dishes on ice. Before irradiation, cells in monolayer were scraped into suspension in fresh, cold medium with a silicone rubber policeman, and gently dispersed; they assumed a rounded shape and appeared as single cells or small groups, as did mitotic cells and cells grown in suspension. Corrections were made for absorption by medium or PBS during irradiation.

Single Cell Survival Experiments

Irradiated cells were plated out in plastic dishes at appropriate dilutions in triplicate for each UV dose. Colonies were fixed, stained, and scored after incubation for 10 d.

Chromosome Isolation and Irradiation

Metaphase HeLa chromosomes from cells prelabeled with [^{3}H]thymidine as above were isolated by the method of Wray (4), in 1.0 M hexylene glycol, 0.5 mM $CaCl_2$, buffered to pH 6.8 with 0.1 mM piperazine-*N*,*N*′-bis-(2-ethane sulphonic acid) (PIPES). Chromosomes in 5 ml ice-cold isolation medium in 150 mm dishes were irradiated on ice. Chromosomes were washed from the dishes with more cold isolated medium, pelleted by centrifugation at 3,000 *g* for 10 min, hydrolyzed, and assayed for dimers.

Dimer Analysis

After irradiation, cells were centrifuged and the pellets extracted twice with ice-cold 5% trichloroacetic acid (TCA). The acid-insoluble pellets were hydrolyzed by heating with 0.6 ml 6M perchloric acid at 100°C for 3 h. The hydrolysates were neutralized with ice-cold 1 M KOH and centrifuged to remove precipitated perchlorate. The supernatant, together with that obtained from a wash of the precipitate with 1 ml cold water, was added to 10 ml of 0.02 M ammonia and applied to a column of Dowex 1 X 8-400 (Sigma Chemical Co., St. Louis, Mo.) converted to the formate form. The sample was followed with 0.02 M ammonia until 10 5-ml fractions had been collected. Cyclobutane pyrimidine dimers were eluted with 0.02 M ammonium formate containing ammonia to bring the pH to 8.8 (10 5-ml fractions collected), and undimerized bases were eluted with 0.02 M formic acid (10 5-ml fractions). This method is due to Sekiguchi et al. (5). Samples of the fractions were counted with Tritosol scintillation fluid (6).

Alkaline Sucrose Sedimentation

Details of the method of alkaline sucrose sedimentation, fractionation of gradients, etc. have been given previously (2). Briefly, the cell suspension was placed on a 2% neutral sucrose layer over a 4.5 ml linear gradient of 5–20% (wt/vol) sucrose, 0.3 M NaOH, 0.5 M NaCl, 0.01 M Na_2EDTA, and immediately centrifuged in an SW50L rotor at 30,000 rpm in a Beckman L2-65B ultracentrifuge (Beckman Instruments, Spinco Div., Palo Alto, Calif.) at 4°C. DNA profiles were obtained from the acid-precipitated [^{3}H]DNA in the fractions of the gradient, measured by scintillation counting.

Light Scattering Measurements

HeLa cells from spinner culture were washed twice in PBS to remove UV-absorbing components of the medium, and resuspended in PBS at 8×10^5 cells/ml. The cell suspensions were placed in 1 cm square quartz cuvettes, and the extinction measured with a Pye Unicam SP1600 spectrophotometer (Pye Unicam Ltd., Cambridge, England) over a range of absorbing (230–320 nm) and nonabsorbing (320–500 nm) wavelengths with 1 nm band width. The method of Latimer and Eubanks (7) was used to compute the scattering contribution: absorption spectra were measured with the cuvettes in the normal position, giving a series of extinctions $E_1\lambda_1$, $E_1\lambda_2, \ldots$, and then with the cuvettes rotated through 90° so that the opalescent sides randomized forward-scattered and nonscattered light, giving a second series of extinctions $E_2\lambda_1$, $E_2\lambda_2, \ldots$. The scattering constant A was then obtained for nonabsorbing regions of the spectrum, λ_0:

$$A = E_2\lambda_0(E_1\lambda_0 - E_2\lambda_0)$$

and then the true extinction due to absorption at any wavelength is:

$$E\lambda_n = E_2\lambda_n - A(E_1\lambda_n - E_2\lambda_n)$$

DNA Estimation

DNA was measured by the diphenylamine method of Burton (8). Samples of a suspension of mitotic-arrested HeLa cells were counted with a Coulter Counter (Coulter Electronics, Inc., Hialeah, Fla.), and the analysis was performed on the DNA precipitated from the suspension with 0.5 M perchloric acid.

A Model for UV Absorption by Eukaryotic Cells

To interpret the cell cycle dependence of UV damage and UV killing, it would be convenient to be able to estimate the UV dose actually absorbed by the cellular DNA at different stages of the cycle.

The amount of UV absorbed by the nucleus will depend on its content of UV-absorbing material; on its state of expansion or contraction, since a uniformly contracted nucleus will offer a smaller target area than a larger one; and on the extent of shielding by cytoplasmic regions closer to the UV source. The amount of absorption by the DNA in the nucleus will also depend on the ratio of DNA to non-DNA UV-absorbing material in the nucleus, and on their respective locations. Similar factors affect UV absorption by different zones of the nucleus. All these factors are probably cycle-dependent for any nuclear target; thus the proportion of incident radiation absorbed by the target must also be cycle-dependent.

BASIC MODEL Direct measurements of UV absorption by components of such complex structures as eukaryotic cells are not easy; we have, however, constructed a simplified computer model, run on an IBM 370/165 (IBM Corp., White Plains, N.Y.), to simulate the effects of variations in target geometry on UV absorption. In the simplest form of this model, the cell is assumed to comprise a series of zones of extinctions $E_1, E_2 \ldots$ bounded by concentric spheres of radii $R_1, R_2 \ldots$; in the simplest case of all, only two zones, nucleus and cytoplasm, are considered (Fig. 1). Parallel radiation of initial intensity I_0 is assumed to pass through the cell; for a ray at distance D from the sphere axis, the path length through the cytoplasm before reaching the nucleus is

$$L_1 = R_2 \sin(\arccos D/R_2) - R_1 \sin(\arccos D/R_1),$$

and the path length through the nucleus is $L_2 = 2R_1 \sin(\arccos D/R_1)$ or, for $D \geq R_1, L_2 = 0$.

Assuming Beer's law to hold, the intensity of radiation at the near surface of the nucleus is $I_1 = I_0 e^{-L_1E_1}$, the intensity at the far surface of the nucleus is $I_2 = I_1 e^{-L_2E_2}$, and the intensity at the far side of the cell is $I_3 = I_2 e^{-L_1E_1}$.

Thus the absorption along this light path by the cytoplasm is $\Delta I_c = I_0 - I_1 + I_2 - I_3$ and the

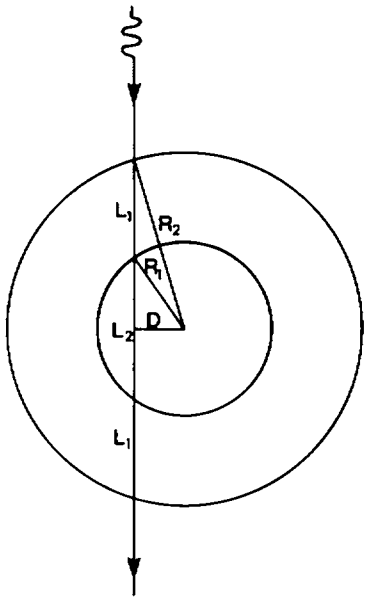

FIGURE 1 Geometry of simply two-zone model of cell.

absorption by the nucleus is

$$\Delta I_n = I_1 - I_2.$$

The computer program calculates values of ΔI_c and ΔI_n for incremental values of D, and derives the total light absorption for all light paths passing through a three-dimensional spherical cell,

$$\sum_{D=0}^{D=R_2} 2\pi D(\Delta I_c),$$

which for small values of increment ΔD is approximately

$$\sum_{D=0}^{D=R_2} \pi[(D + \Delta D)^2 - D^2](\Delta I_c)$$

and the total nuclear absorption

$$\sum_{D=0}^{D=R_1} 2\pi D(\Delta I_n),$$

or approximately

$$\sum_{D=0}^{D=R_1} \pi[(D + \Delta D)^2 - D^2](\Delta I_n)$$

A similar approach can be used for a three-zone model (central euchromatin, surrounded by heterochromatin, surrounded by cytoplasm), or a four-zone model with very dense membrane-asso-

ciated chromatin between heterochromatin and cytoplasm (9); we have assumed the membrane-associated chromatin to be of the same packing density as metaphase chromosomes. In each case if the contribution of DNA absorption to the total extinction of each zone is known, the total absorption of UV by DNA can be derived.

The program calculates, for each of a series of zones for incremental values of D, the target area of that zone and the fraction of the radiation absorbed by any component of that zone. As the absolute value of the incident irradiance is not specified, the total absorption is not in absolute terms but is relative to the UV incident on unit area; we have used cell dimensions in micrometers, so the calculated absorption by a model cell, or nucleus, may conveniently be expressed in terms of joules of UV absorbed per joule incident per square micrometer. If there were no change in the photoreactivity of DNA through the cell cycle, the formation of photodimers would be related to the specific absorption of UV by the DNA, which can be expressed as joules absorbed per picogram DNA per joule incident per square micrometer.

ELABORATION OF THE MODEL In constructing this model, it is assumed that (*a*) Beer's law applies, (*b*) the cell has spherical symmetry, (*c*) light scattering is negligible, and (*d*) all cells are equivalent; all these assumptions need qualifying.

(*a*) The absorption of UV by droplets of concentrated DNA and by lymphocyte nuclei was found by Lindström et al. (10) to depart from Beer's law for unexplained reasons; they report a dependence of apparent extinction coefficient on DNA concentration, with the coefficient equal to $2.49 - [0.5 \log_{10}(\%\ \text{DNA})]\ \text{pg}^{-1}\mu\text{m}^2$. We have used this relationship in some model calculations.

(*b*) An interphase cell grown in suspension culture does have approximately spherical symmetry of UV-absorbing material, neglecting the nucleoli, but mitotic cells do not. Initially we assumed that the mitotic chromosomal material is homogeneously mixed with an equal volume of cytoplasmic material, and occupies a central spherical zone. This is not a very plausible model and probably underestimates mitotic absorption (see Results). We have used a variant of the model for computing absorption by more realistic mitotic cells, considering the chromosomes as lying within a broad, short cylinder with a central hollow cylinder free from chromosomes, of dimensions corresponding to the size of the mitotic plate. As the chromosomes occupy only part of the volume of such a plate, it is necessary to correct for the "sieve effect" whereby some UV will pass through the plate without striking any chromosomes. The apparent extinction of a suspension of particles, E_s, and the extinction of individual particles, E_p, are related by the equation given by Latimer and Eubanks (7): $E_s = P(\log_{10}e)(1 - 10^{-E_p})$, where P is the projected area of all particles in the light path. It is necessary to compute P for each simulated light path through the plate, and to derive E_s as a function of E'_p, being the difference between the extinction of the chromosome, E_p, and the extinction of the cytoplasmic matrix, E_c. Then the proportion of the total extinction attributable to chromosomal material for any one light path through the plate is $[E_s + E_c(V_p/V_c)]/(E_s + E_c)$, where V_p, V_c are the volumes of the chromosome set and of the total plate, respectively.

Calculating absorptions for the various possible orientations of this plate would demand much computer time, so we have calculated only the extreme cases with plates parallel and perpendicular to the incident light. The absorption with the plate perpendicular is greater than in the parallel case by a factor of 50–100%, dependent on the plate dimensions so we have assumed that the average value for a population of randomly oriented cells lies somewhere near the average of the extreme cases. Since chromosomes in nitrous oxide-arrested HeLa as viewed by Nomarski optics take up a variety of arrangements, we have calculated the possible specific absorptions per picogram of DNA for a range of dimensions.

(*c*) UV passing through a cell is not just absorbed; it is also reflected, refracted, and diffracted. Though microspectrophotometric measurements on single rat fibroblasts (11), chick fibroblasts (12), and lymphocytes (10) indicate that UV scattering is small compared to absorption, Chu (13) reported that UV scattering in Chinese hamster cell suspensions is much greater than absorption. We find, after making appropriate corrections, that 37% of the light loss from bulk suspensions of HeLa irradiated at 254 nm can be attributed to scattering (see Results). Nevertheless, we believe

that nonabsorptive effects can be neglected in our calculations for the following reasons. The scattering of 500 nm light by cells is predominantly within 5° of the incident beam (14). With UV of shorter wavelength, the amount of scattering would be greater, but the position of maximum scattering intensity would be even nearer the incident beam (15). Deviation of this order would not greatly affect the computed path lengths. Furthermore, most of this forward scattering can be attributed to the perimeter of the cell (16, 17) and thus affects only light that would not pass through the inner nuclear zones. Calculations indicate that only the high-angle scattering, of an intensity about 10^{-3} of the forward scattering, can be attributed to cell nuclei (18). Thus, fortunately, it was not necessary to attempt to compute scattering factors for rough-surfaced, internally inhomogeneous cells of uncertain refractive index.

(*d*) HeLa is a heteroploid line. The model involves calculations for one cell of average size; but since absorption is not a linear function of cell size, the average absorption per cell would differ from the absorption of the average cell, by a quantity we have disregarded. Also, HeLa cells do not keep perfect synchrony after release from even a double cycle block; hence the calculated dependence of absorption on cell cycle time will show sharper transitions than would actually be observed in a population of cells.

DISTRIBUTION OF ABSORBING MATERIALS IN THE MODEL CELL The extinction coefficients for the various zones of the model cell are not directly accessible. We have taken cytological data for the cell cycle dependence of the amounts of nuclear and cytoplasmic non-DNA UV-absorbing materials in L cells from Killander and Zetterberg (18) and Zetterberg (19). In this cell line, nuclear non-DNA absorption declines slightly through interphase; cytoplasmic absorption rises considerably. We have assumed that the distribution of non-DNA absorbing materials in HeLa cells is similar, and that their amounts are proportional to the amounts of DNA per cell; we have adjusted the rates of change of amount of material to allow for different durations of cell cycle phases, assuming that the total relative change through any one phase is the same in HeLa as in L cells. The published data give values for various stages of the cycle; we have interpolated values to obtain data for times intermediate between those studied. Mitotic cells were not studied by Zetterberg; we have assumed that in mitosis all non-DNA UV-absorbing material (predominantly RNA) leaves the chromosomes. The distribution of non-DNA-absorbing material within the nucleus may be assumed to be uniform, or else preferentially concentrated in the inner euchromatin zone. The amount of DNA per cell may in the simplest case be assumed to increase linearly through S phase from the experimental value of 9.3 pg/cell after division; we have also allowed for restriction of replication to the heterochromatin shell in the latter period of S phase (20) and for a maximal rate of DNA synthesis in the central hour of S phase as reported for HeLa cells (21, 22). The volumes of the nuclear zones, on which the concentrations of absorbing substances and hence the extinctions depend, were estimated initially by taking the cycle-dependent expansion factors for core euchromatin and shell heterochromatin relative to mitotic chromosomes observed by Dewey et al. (23) for Chinese hamster Don cells, and used for their calculations of the dependence of X-ray sensitivity on chromatin expansion; and taking Du Praw's (24) value of 0.256 g/ml for the density of DNA in mitotic chromosomes. The expansion factors were adjusted to allow for different lengths of cycle phases, and factors for intermediate times interpolated. However, it appears that nuclear expansion is much greater in HeLa than in Don cells; the maximum volume calculated for interphase HeLa nuclei using the chromatin expansion factors of Dewey et al. (23), which give a maximum expansion factor of 2.63 relative to mitotic material, is about 240 μm^3, whereas visualization of our HeLa line in random interphase by Nomarski optics indicates nuclear volumes of 300–1200 μm^3. We therefore increased the expansion factors of Dewey et al. (23) to allow for this; in various computer runs the extra expansion was either supposed to be uniform throughout the nucleus or attributed only to the inner core. The cell volume was calculated by taking an initial cell volume at metaphase of 2800 μm^3, derived from microscopic measurement, and assuming a 50% decrease, through a 1-h mitotic period, followed by linear or exponential growth to the end of the cycle. Volumes of nuclear and cytoplasmic zones, and the concentrations of UV-absorbing materials in them, were calculated at 30 min intervals through a simulated HeLa cell cycle of 15 h (5 h G_1, 7 h S, 3 h G_2).

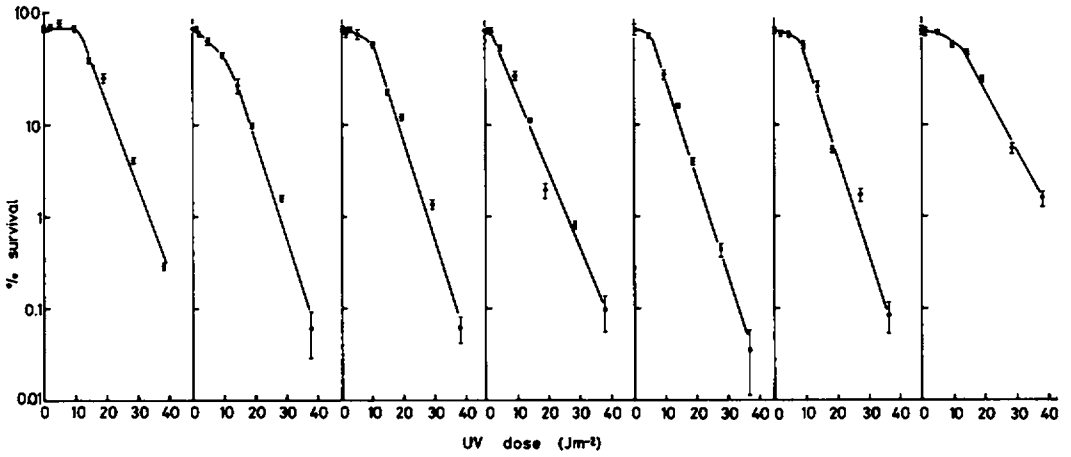

FIGURE 2 UV survival curves of synchronized HeLa cells at different stages of the cell cycle. The data points represent the mean ± SEM for each triplicate set of plates. The linear portion of each curve was fitted by eye. HeLa cells were reversibly synchronized in metaphase by high-pressure nitrous oxide treatment and their interphase progeny have an absolute plating efficiency of 20–27%.

RESULTS

Survival Studies: Cycle-Dependence of UV Resistance

Fig. 7 gives details of the cell cycle after release of reversibly arrested mitotic HeLa cells from a nitrous oxide pressure block. The amount of DNA synthesis in the population at various times after release was estimated by scintillation counting after pulse labeling with [^{3}H]thymidine. The proportion of cells in S phase, monitored by autoradiography, closely followed the pattern of [^{3}H]thymidine incorporation into TCA-insoluble material (data not shown). The mitotic index was measured after colcemid accumulation.

The relationship between position in the cell cycle and cell survival after UV irradiation is shown in Fig. 2. Survival curves were plotted against UV dose for cells irradiated at seven points in the cycle. From these curves we obtained the shoulder width (D_q) and mean lethal dose (D_0). The variations in D_q and D_0 (from four cell cycle experiments) are presented in Fig. 3 as convenient indices of UV-resistance. Populations of cells in late G_1–early S phase appear to be most sensitive to UV irradiation. Although the mean lethal dose does not change dramatically during the cycle the shoulder width does. Mitotic and late S–G_2 cells have the greatest shoulder and late G_1–early S phase cells the smallest.

Sedimentation of DNA in Alkaline Sucrose Gradients

Having shown that the probability of surviving a given dose of UV varies with the position of the irradiated cell in the cell cycle, we looked for variations through the cycle in the overall conformational response of DNA to UV irradiation. This response was measured in terms of the sedimentation behavior of DNA on alkaline sucrose gradients.

The conventional method of alkaline sucrose gradient sedimentation has generally proved inadequate to resolve any changes in DNA structure caused by UV irradiation or UV-induced excision repair in mammalian cells (see reference 25 for a review), probably because

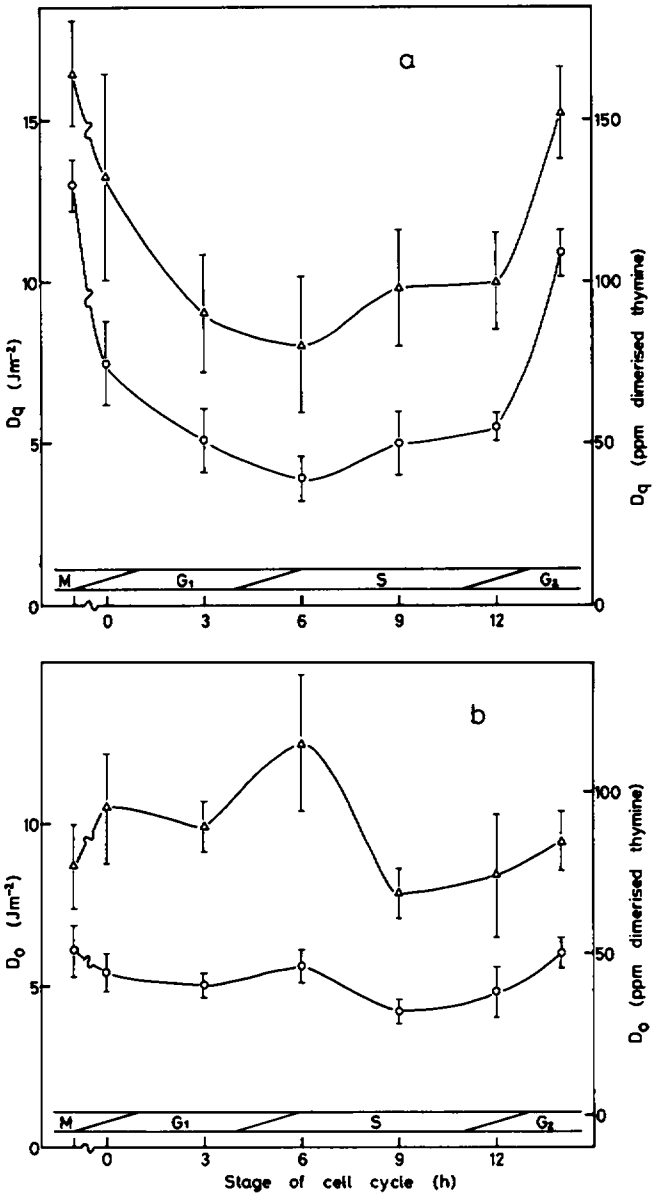

FIGURE 3 Cycle dependence of survival parameters of UV-irradiated HeLa cells. Data points represent mean ± SEM for quadruplicate synchronized cell cycles; Points —○— show (*a*) D_q and (*b*) D_0 in terms of joules per square meter administered, points —△— show (*a*) D_q and (*b*) D_0 in terms of parts per million [^{3}H]thymine converted to pyrimidine dimers, calculated from data shown in Fig. 7.

such changes are not visible in completely denatured molecules, or because they are obscured by the considerable breakage of DNA during prolonged alkaline lysis. Cleaver (25) was able to show the effect of UV on DNA in unsynchronized human fibroblasts by a technique in which cells experienced only brief lysis before centrifugation. We have developed a method similar to this, in which the lytic time is reduced still further. Cells (previously

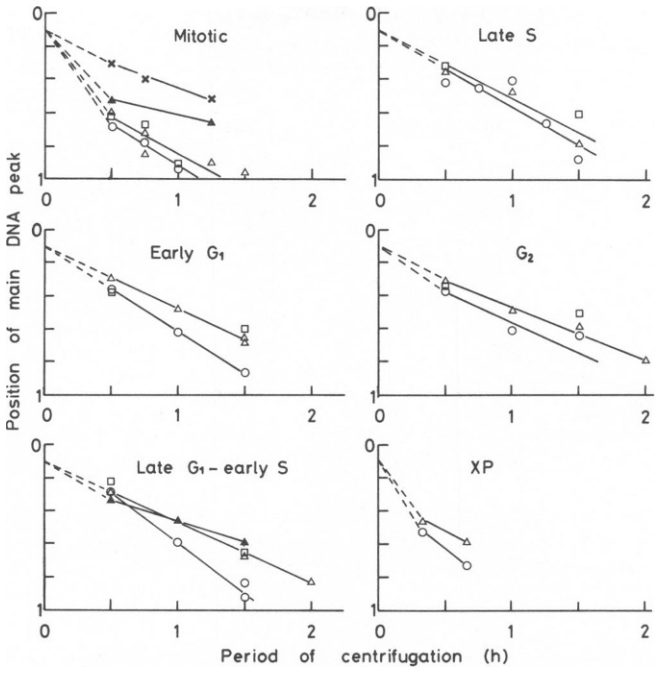

FIGURE 4 Position of sedimenting DNA as a function of the period of centrifugation. Synchronized HeLa cells (in mitosis and in interphase at the stages indicated) and random xeroderma pigmentosum (XP) cells, prelabeled with [^{3}H]thymidine, were centrifuged on alkaline sucrose gradients for various times. The position of the main DNA peak is plotted on a linear scale from 0 (top of gradient) to 1.0 (bottom of gradient). —○—, no UV; —△—, cells irradiated with UV (144 Jm^{-2}); □, cells irradiated with UV (144 Jm^{-2}) and incubated at 37°C for 45 min (lines not drawn); —▲—, cells irradiated with UV (430 Jm^{-2}); —x—, cells irradiated with UV (1,440 Jm^{-2}). The lines are those used to estimate the sedimentation coefficients listed in Table I.

labeled with [^{3}H]thymidine) are placed on a neutral sucrose layer on top of the alkaline gradient and centrifuged immediately, so that no lysis occurs before centrifugation; under these conditions, DNA begins sedimentation in a double-stranded form, and it is likely that as the DNA moves into the alkaline zone, it is only slowly converted to the single-stranded form (25–28). UV-induced structural modifications of DNA should influence its sedimentation behavior by altering the rate of separation into single strands (28). This technique has proved useful in detecting the effects of inhibitors of DNA synthesis on UV-induced repair (2, 29); such agents cause slowing of sedimentation of prelabeled DNA. The method also reveals cell cycle dependence of sedimentation rates and coefficients, and effects of UV irradiation alone, as is shown in Fig. 4 and Table I. Whereas the DNA of unirradiated interphase cells sediments linearly with time, mitotic DNA has a biphasic pattern, an initial phase of rapid movement being followed by a slower, linear sedimentation. Irradiation with UV generally causes a slowing of DNA sedimentation, in synchronized HeLa cells or in xeroderma pigmentosum cells (unsynchronized). The greatest relative effect of UV in HeLa cells is seen in cells at late G_1–early S.

It is important to consider whether the slowing of sedimentation is an effect of UV irradiation alone, or whether it results from the enzymic process of excision repair, induced by

TABLE I

SEDIMENTATION OF DNA ON ALKALINE SUCROSE GRADIENTS

Cell type	Stage in cycle	Sedimentation coefficient		
		Control (no UV)	+UV ($144\ Jm^{-2}$)	+UV ($430\ Jm^{-2}$)
HeLa	Mitosis*	>495	>460	>365
		220	190	80
	Early G_1	220	165	—
	Late G_1–early S	260	160	110
	Late S	200	175	—
	G_2	160	140	—
Xeroderma pigmentosum	Random	260	170	—

*Sedimentation coefficients refer to the first rapid phase of sedimentation and the second slower phase.

Sedimentation rates were calculated from the positions of DNA peaks after centrifugation for various times, and sedimentation coefficients were calculated by reference to the sedimentation rate of X-irradiated Chinese hamster ovary marker DNA (165S) (77).

UV, despite the precautions taken to maintain irradiated cells at low temperature and to transfer them to the gradients as soon as possible. In a control experiment irradiated or unirradiated HeLa cells were loaded directly on to gradients, without the washing stage, and thus the interval between irradiation and centrifugation was shortened by about half. The slowing of sedimentation of DNA caused by irradiation was unaltered, in spite of the reduced opportunity for excision repair. It is of interest that xeroderma pigmentosum cells, from a culture with much reduced unscheduled DNA synthesis (30), showed a similar effect of UV on DNA sedimentation, implying that slower sedimentation is a direct effect of radiation. However, neither of these controls excludes the possibility that excision repair contributes to the slowing of sedimentation, since there is a report of enzymic breakage of UV-irradiated DNA in bacteria chilled in ice immediately after irradiation (31) and there are also indications of UV specific endonuclease activity in xeroderma pigmentosum cells (2, 32–34).

Incubation of cells at 37°C for 45 min after irradiation with UV ($144\ Jm^{-2}$) to permit excision and repair, results in sedimentation profiles which tend to be broadened, flattened, and shifted towards the top of the gradient compared with those from unincubated cells, though these tendencies are not necessarily present to the same extent (or at all) in all experiments. Fig. 5 shows examples of profiles for cells at mitosis and in interphase. The breadth of the peaks makes estimation of their position less meaningful; however, these positions are indicated on Fig. 4. (Note that the biphasic pattern of sedimentation of mitotic DNA is not altered by incubation for 45 min.) The changes in sedimentation that occur on incubation after UV, although slight, are consistent with the occurrence of more radical disruption of DNA conformation and size during excision repair.

The recovery of DNA from the gradient in these experiments is rarely higher than 70%; some DNA apparently sediments very rapidly to a pellet, and the content of the main peak continues to decrease as sedimentation proceeds. Possible explanations for this phenomenon

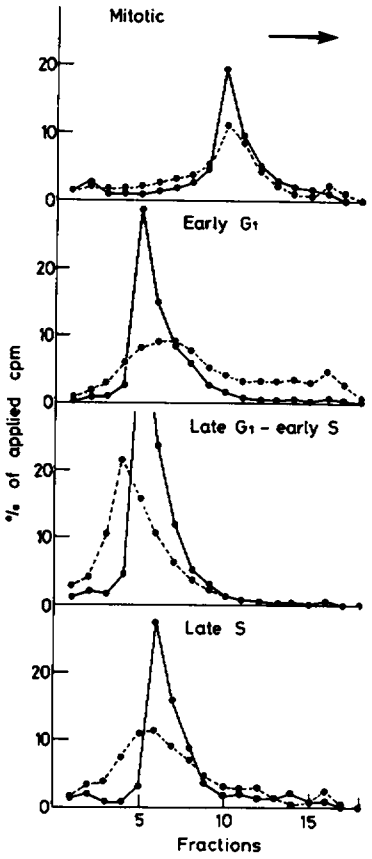

FIGURE 5

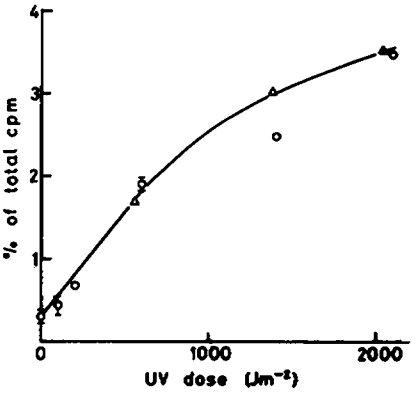

FIGURE 6

FIGURE 5 Effect on DNA sedimentation of incubation after UV irradiation: sedimentation profiles of synchronized HeLa cells (in mitosis and in interphase at the stages indicated). Solid lines, cells irradiated with UV (144 Jm^{-2}); broken lines, cells irradiated with UV (144 Jm^{-2}) and incubated at 37°C for 45 min. The period of centrifugation was 0.5 h.

FIGURE 6 UV dose dependence of dimer formation in unsynchronized HeLa cells. ^3H in the dimer peak is contributed by both $\widehat{TT}$ and $\widehat{CT}$, but as the ^3H originated in [^3H]thymidine the contribution from $\widehat{TT}$ is double with respect to that from $\widehat{CT}$. Triangles and circles represent experiments with different cell populations. Circles with range-bars indicate the average of duplicate samples from a single irradiated population.

will be discussed elsewhere; for the time being we rely on the consistent behavior of the main peak of DNA.

Photochemical Damage Measured by Dimer Formation

A more direct measure of the photochemical damage incurred by the DNA is the formation by UV of cyclobutane pyrimidine dimers. To examine the dependence of dimer formation on UV dose, [^3H]thymidine-labeled, unsynchronized HeLa cells were irradiated with several doses of UV, and the dimer content of their DNA was analyzed chromatographically. Fig. 6 shows the yield of labeled dimers as a percentage of the total recovered tritium, and indi-

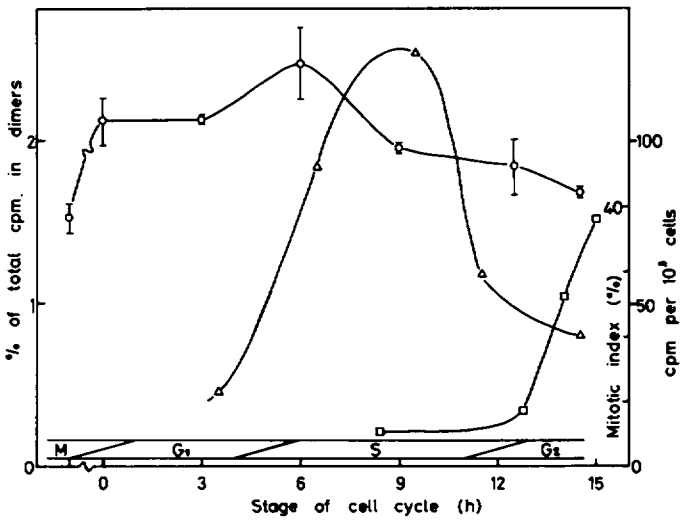

FIGURE 7 Dimer formation as a function of the cell cycle. HeLa cells of a single synchronized cell population, prelabeled with [^{3}H]thymidine, were irradiated in PBS (1,200 Jm^{-2}) at different stages in the cell cycle and assayed for cyclobutane pyrimidine dimers (—○—). Bars indicate range of values of duplicate, or SEM of triplicate samples (separately irradiated). At 6 h after the start of G_1, samples of cells were removed to Petri dishes and incubated with colcemid (Gibco Bio-Cult Ltd., Paisley, Scotland) (0.1 μg/ml). At intervals, cytocentrifuge preparations were made from these samples and the mitotic index was assayed (—□—). DNA synthesis was measured in a separate (unlabeled) synchronized population, by incubating samples with [^{3}H]thymidine (20 Ci/mmol, 1 μCi/ml) for 30 min, and measuring the ^{3}H incorporated into acid-insoluble material by scintillation counting (—△—). The indicator strip along the base of the figure shows the approximate duration of the phases of the cell cycle ascertained from autoradiography after [^{3}H]thymidine pulses as above, in various experiments; by about 5 h after the start of G_1, 30% of cells are in S phase.

cates that at the higher doses dimer formation departs from linearity. There is a small peak of apparent dimers even in material from unirradiated cells; this is regarded as background and the corresponding percentage has been subtracted from the dimer yields in the cell cycle study below.

Measurements of dimer formation at a constant dose of UV (1,200 Jm^{-2}) were made at representative points throughout the cell cycle (Fig. 7). Mitotic cells show the lowest yield of dimers, and there is a dramatic increase in the efficiency of dimer production at the start of G_1 phase. The yield is highest in late G_1 to early S phase and thereafter declines towards the next mitosis. (Over the range of dimer yields measured here, the departure from linearity of dimer formation—see Fig. 6— is small.) We have found similar patterns of dimer formation in previous unpublished series of experiments with HeLa cells; invariably the lowest yield occurs in mitosis.

This cycle dependence of dimer yield means that the survival curves for cells at different stages of the cycle, measuring percentage survival against UV dose given, are not directly comparable, since the number of lesions is a varying function of the dose. It is instructive to express the $D_q s$ and $D_0 s$ of the survival curves in terms of percentage thymine dimerized (Fig. 3).

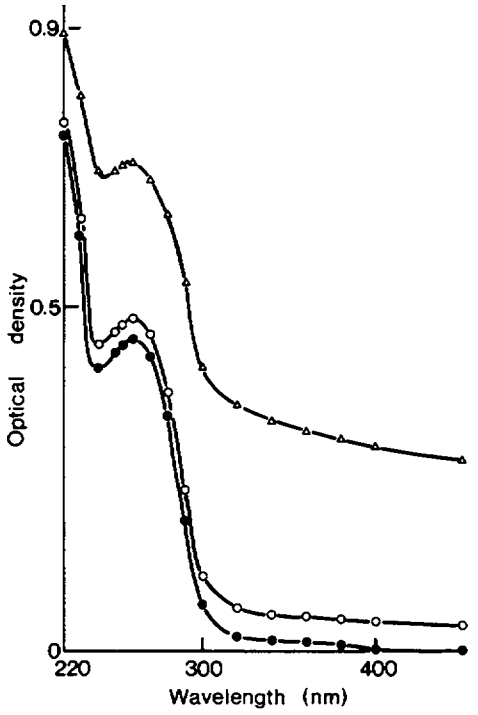

FIGURE 8 Absorption and scattering spectra of HeLa cells in suspension. Random population of HeLa cells at 8×10^5/ml in PBS. —△—, combined absorption and scattering spectrum; —○—, spectrum with correction for forward scattering; —●—, absorption spectrum.

Light Scattering

The extinction spectrum of suspended HeLa cells shows a maximum at about 260 nm and a further increase towards 220 nm, attributable to nucleic acid and protein absorption, and a considerable amount of extinction outside the absorption range, decreasing with increased wavelength, due to scattering (Fig. 8, top curve). The spectrum measured through the opalescent face of the cuvette, in effect corrected for forward scattering since both nonscattered and scattered light leaving the cuvette will be randomized (35), shows much-diminished nonabsorption effects (Fig. 8, middle curve); the corrected absorption spectrum (7) shows absorption peaks responsible for more than half the light loss below 280 nm (Fig. 8, bottom curve). At 254 nm 63% of the total light loss is attributable to absorption.

Computer Simulation of UV Damage

Calculations using the model described above show that the absorption of UV by HeLa DNA varies through the simulated cell cycle. The total absorption by DNA is at a minimum at the end of mitosis, increases through G_1 and S to a maximum at the end of S, and falls rapidly through G_2. Specific absorption per unit mass of DNA, however, reaches a maximum shortly after the G_1–S boundary, then declines slowly through S and more quickly through G_2. The incroporation of the density-dependent DNA absorption of Lindström

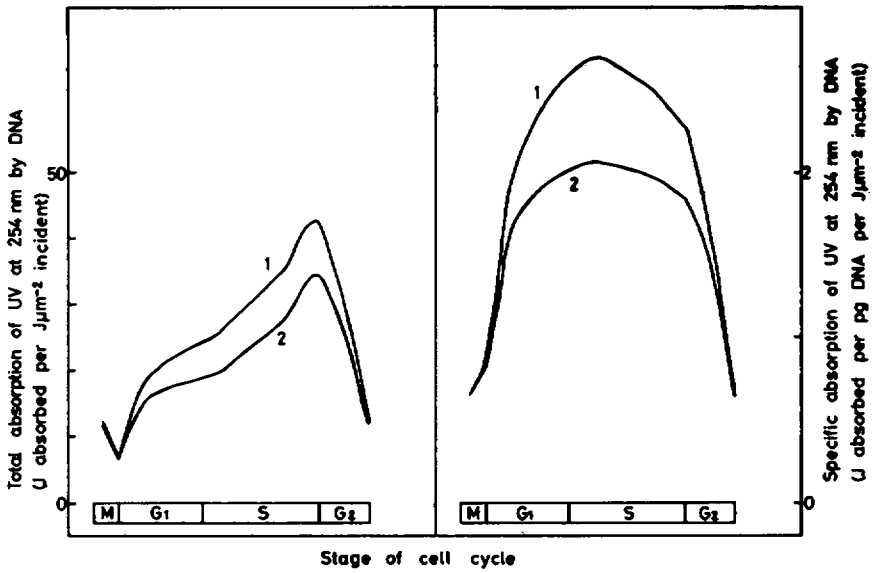

FIGURE 9 Computed absorptions of UV by model cell. Left, total absorption by DNA; right, specific absorption per pg DNA. Calculations were performed with an incremental value of D of 0.02 μm, assuming density-dependent DNA extinction coefficient (curve 1) or constant DNA extinction coefficient (curve 2), exponential increase in cell volume through interphase, DNA synthesis maximal in central S phase, uniform distribution of RNA through the nucleus, and a simple central distribution of mitotic chromosomes.

et al. (10) into the model increases the amplitude, but does not change the shape of the cycle dependence (Fig. 9). The positions of these maxima and minima are fairly insensitive to changes in the simulated cell-cycle parameters, though the absolute values vary (Table II). Calculations varying different parameters indicate that the predominant influences are the expansion and contraction of chromatin and the replication of DNA: cytoplasmic shielding decreases the nuclear absorption by up to 40% throughout the cycle, and nuclear non-DNA absorption decreases DNA absorption by about 15%. Changes in the simulated RNA distribution do not greatly affect the total DNA absorption (Fig. 10).

The specific absorptions of UV by DNA in the simulated inner and outer zones of the nucleus show similar cycle dependence, and are not greatly different in amount. Even with compact nuclei, the outer zone is not likely to have more than 30% more specific absorption than the inner; and if one assumes the DNA absorption coefficient to be concentration-dependent (10), an inner diffuse zone may have a slightly higher specific absorption than the compact outer shell. Similarly, simulations involving a third nuclear zone of dense peripheral membrane-associated chromatin, which may be the most vulnerable target for ionizing radiation (36), did not show outstanding differences in extent or cycle dependence between the absorption of DNA in this region and that in the rest of the nucleus. The specific absorption by the simulated membrane-associated DNA was greater than that of the average DNA by up to 30% (as would be expected from its peripheral position) with a maximum in early S.

TABLE II

DEPENDENCE OF MAXIMA OF COMPUTED SPECIFIC UV ABSORPTION ON SIMULATED CELL-CYCLE PARAMETERS

Cell cycle	Density-dependent DNA extinction coefficient		Density-independent DNA extinction coefficient	
	Maximum specific absorption	Time after mitosis of maximum	Maximum specific absorption	Time after mitosis of maximum
	J absorbed/ pg DNA per Jμm^{-2} incident	*h*	*J absorbed/ pg DNA per Jμm^{-2} incident*	*h*
A	2.66	7	2.04	7
B	2.45	6.5 or 7	1.92	7
C	2.83	7	2.13	7
D	2.65	6.5	2.03	6.5
E	2.63	6.5	2.02	6.5 or 7
F	2.63	6.5	2.02	6.5
G	2.58	7	1.99	7
H	2.67	7	2.06	7
I	2.44	7	2.01	7
J	2.80	8	2.14	7.5 or 8

Specific UV absorptions per picogram of DNA were computed at 30-min intervals through simulated HeLa cell cycles; time and value of maxima are shown. Unless otherwise stated, calculations assumed exponential cell volume increase, 5 h G_1, 7 h S, and 3 h G_2 phases, uniform distribution of nuclear non-DNA absorbing material, cycle-dependent nuclear volume change uniformly five times as great as in Chinese hamster Don cells, 25% of DNA in central core, and either density-dependent or density-independent DNA extinction coefficients. Conditions varied in different computations were: cycle A, assuming DNA replication maximal mid-S phase; cycle B, like A but with cycle-dependent nuclear volume change four times as great as in Don cells; cycle C like A but with cycle-dependent nuclear volume change six times as great as in Don cells; cycle D like A but with no DNA replication; cycle E, like A but with DNA replication uniform through S phase; cycle F like E but with 75% of DNA in core; cycle G like E but with 99% of DNA in core; cycle H like A but with linear increase in cell volume; cycle I like A but attributing all cycle-dependent nuclear volume change to changes in core volume; cycle J like A but allowing 7 h for G_1 phase.

The absorption of UV by simulated cytoplasm increases steadily through the cell cycle: the specific absorption hardly changes, being slightly higher in early G_1 than elsewhere.

The amount of absorption attributed to DNA in the mitotic model cell depends on the configuration postulated for the chromosome set; the calculations described above employ a spherical model configuration which underestimates mitotic absorption. We have therefore calculated absorption for chromosomes arranged in metaphase plates. The results are rather sensitive to the assumed plate size; the computed absorptions increase with simulated plate radius and thickness, decrease with the size of the central chromosome-free cylinder, and to a smaller extent increase with the number of independent absorbing centers that the chromosomes are supposed to represent. The average specific absorptions for plates of the dimensions observed in our HeLa using Nomarski optics (radius of plate 4.5–6 μm, thickness 2–4 μm, radius of central chromosome-free zone 1.5–2.5 μm) vary from 0.7 to 1.6 J absorbed/J μm^{-2} incident: substantially below the peak interphase values.

A check on this range of values is provided by comparing dimer yield in isolated chromosomes (relative to that in intact mitotic cells) with the calculated specific UV absorptions for

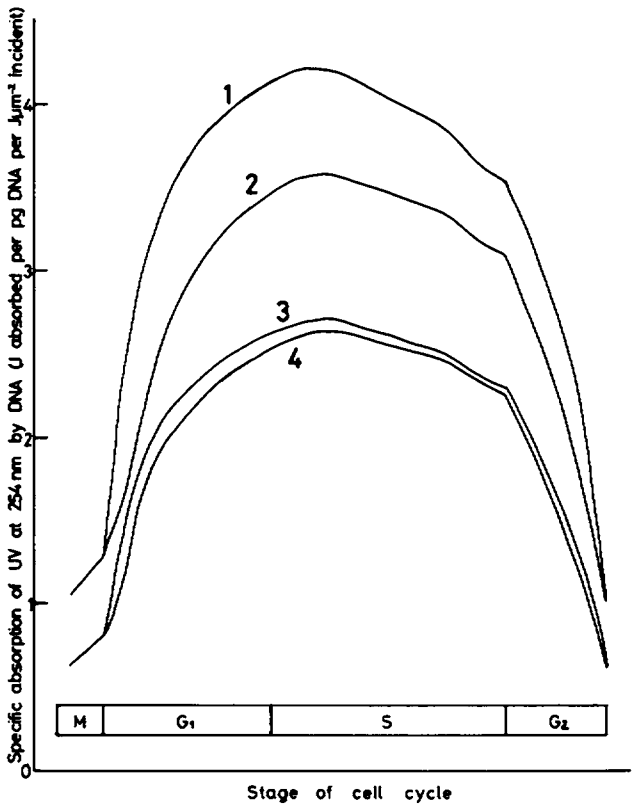

FIGURE 10 Dependence of computed DNA specific absorption on simulated distribution of non-DNA UV-absorbing material. Calculations were performed as in Fig. 9 except that curve 1 assumes no non-DNA UV-absorbing material in cell; curve 2 assumes no UV-absorbing material in cytoplasm; curve 3 assumes all nuclear non-DNA UV-absorbing material confined to peripheral zone with 25% of DNA; curve 4 assumes all nuclear non-DNA UV-absorbing material confined to central zone with 75% of DNA.

simulated isolated chromosomes (relative to that in simulated mitotic cells). We find that the dimer yield for isolated chromosomes in nonabsorbing isolation medium is approximately three times that for mitotic cells given the same incident UV dose in nonabsorbing saline solution; the simulated "chromosomes" have a specific UV absorption of 3.0–3.5 J absorbed/pg DNA per J μm^{-2} incident, depending on the amount of DNA they are supposed to contain. So unless the photoreactivity of isolated chromosomes is changed by the isolation procedure, the specific UV absorption of chromosomes in cells would by this criterion be about 1.0–1.2 J absorbed/pg DNA per J μm^{-2} incident.

DISCUSSION

Ultraviolet light is both a mutagen and a carcinogen. There is now considerable evidence that the most critical UV target is the chromatin. Analysis of UV action spectra for yield of chromosome aberrations and cell killing indicates that both nucleic acids and chromatin proteins are involved (13, 37). The physical state of chromatin varies not only among dif-

ferent cell types (38) but also during the cell cycle (39–44). We have previously found (42) that the decondensation of chromatin after UV irradiation is cycle dependent, and temporally associated with changes in the rate of repair DNA synthesis. It is clear that the organization of chromatin should be considered as a major factor in the interaction between UV and the cell. Changes in the molecular organization of chromatin may affect the photoreactivity of the DNA; changes in the distribution of chromatin and other UV-absorbing materials in the cell may affect the amount of UV reaching the DNA; either of these would affect the rate of formation of lethal lesions. In this paper we are primarily concerned with an examination of the varying efficiency with which UV light introduces photochemical lesions into DNA as a function of changes in the organization of chromatin in the cell cycle. This information will provide a basis for further studies on the rate and efficiency of the various repair processes in different parts of the cycle and will enable a more precise estimate to be made of the relation between initial UV damage, chromosome aberrations, cell survival and mutagenesis.

The best characterized effect of UV on DNA is the formation of cyclobutane pyrimidine dimers (45). We find that the efficiency of dimer production is apparently lower than previously reported; after irradiation with 1200 Jm^{-2}, between 13 and 21 ppm thymidine/Jm^{-2} is converted to pyrimidine dimers ($\widehat{CT}$ & $\widehat{TT}$) at different stages of the cycle. This compares with reported values of 83 ppm (46) or 45 ppm (47) or 40 ppm (48) thymine converted to pyrimidine dimers per Jm^{-2} of UV at 254 nm, in random unsynchronized HeLa; of 22 ppm thymine converted to thymine-thymine dimers per Jm^{-2} in random unsynchronized HeLa (49), and of 37 ppm to 70 ppm thymine converted to pyrimidine dimers per Jm^{-2} at different stages of the cycle of synchronized HeLa (50). Some discrepancy would be expected from differences in the conditions of irradiation. Shielding of cells by different media will vary, but HeLa cells irradiated in phenol red-free PBS (49, this paper), or Hanks' buffered saline solution (47, 50) should be less shielded than cells irradiated in Hanks' buffered saline solution with phenol red (46). Irradiation of monolayer cells (46–48, and interphase cells in reference 50) should produce a higher dimer yield, owing to the flattening of the cells, and loss of cytoplasmic shielding (Fig. 10), than irradiation of suspended, spherical cells (49, this paper and mitotic cells in reference 50). But these considerations do not account for the variations. We are confident that our results are not due to instrument error; the radiometer calibration has been checked by the National Physical Laboratory, Teddington, and found to be accurate to within 4%.

The efficiency of dimer formation relative to incident dose is cell cycle-related. In metaphase the production of dimers per unit DNA is least efficient. With entry into G_1, however, the efficiency rises sharply, and increases through G_1 to reach a maximum in populations of cells in late G_1–early S, and then declines in late S and G_2 towards the lower level found in mitotic cells.

There have been few previous studies of dimer production in synchronized mammalian cells. In Chinese hamster B14 cells, Steward and Humphrey (51) found that at doses up to 10^3 Jm^{-2} 34% more dimers were produced in cells irradiated in S phase than in G_1, while Trosko et al. (52), irradiating Chinese hamster cells at 265 nm, found 20% more dimers in early S phase than in G_2. Watanabe and Horikawa (50) studied five points in the HeLa S3 cycle, including mitosis, and found two peaks of dimer production, one in mitosis and a

greater one in mid S phase; they report a 40% decrease in dimer yield between mitosis and G_1—in marked contrast with our findings.

UV killing has generally been found to be greatest in late G_1–early S phase, in human D98/A_9 (53), Chang liver (54) and HeLa cells (this study); in Chinese hamster V79 (55) and CHO-K1 cells (29); and in mouse L cells (56). Contrary reports indicate greatest killing in mid-S phase in HeLa (57) and V79 (58), or in mid G_1 and in late S phase in HeLa (59). The changes reported here in the general shapes of the UV survival curves during the HeLa cell cycle agree with the other published study of synchronized Hela survival curves (57).

In addition to the measurements of dimer yield, we have examined the overall effect of photochemical damage on the conformation of cellular DNA, by means of a modified alkaline sucrose sedimentation technique. The principal effect of UV on the behavior of DNA on the minimal lysis alkaline sucrose gradients is a dose-related slowing of sedimentation, the maximum reduction in sedimentation rate being seen in late G_1–early S populations, at the time of maximal specific UV absorption according to our model and at the time of maximal dimer yield. Changes in sedimentation rate under alkaline conditions indicate changes in conformation or size of the DNA. These may be the result of rapid repair nuclease activity after UV irradiation, introducing single-strand DNA gaps; as explained above, we have been unable to exclude this possibility, which has been offered by Cleaver (25) to explain a similar effect. Alternatively, the sedimentation changes may result directly from the photochemical lesion; it is known that UV induces local regions of denaturation, and other conformational changes, in DNA (60–66), and an extrapolation of the work of Brent (67) on phage DNA suggests that some single-strand breaks may be induced nonenzymically in DNA at the UV doses used here. Local regions of denaturation or a few single strand breaks may serve as starting points for partial strand separation in alkali, resulting in slower sedimentation.

The cycle dependence of photoproduct formation might be due to changes in the geometry or the photoreactivity of the cell DNA, or both. Our computer simulations of absorption show that it is possible to account for both the extent of variation of dimer yield, and the position of the minimum in mitosis and the maximum at the beginning of S, largely in terms of plausible changes in the target geometry and consequent changes in the specific absorption of UV by DNA. The computer simulations are a hypothetical exercise, not a proof. The parameters of the model are not sufficiently well-defined to confirm or rule out some contribution from changing photoreactivity. For isolated DNA, the qantum yield of photodimers is about 40% higher for the single- than for the double-stranded form (68) and the abundance of single-stranded DNA in chromatin is reported to be maximal in S phase (69); however, nothing is known about the photoreactivity of protein-complexed single-strand DNA in chromatin. The dimer yield maximum in mitosis reported by Watanabe and Horikawa (50) could perhaps be explained if the chromosomes in their mitotic preparations were far more widely dispersed through the cytoplasm than is the case in our HeLa strain.

The computed UV absorptions by central and peripheral regions of the nucleus do not support the attractive suggestion of Hsu (70) that the peripheral, genetically inactive heterochromatin shields the central euchromatin, at least as far as UV is concerned. The model computations are also relevant to various experiments on the localization of repair synthesis of DNA in UV-irradiated nuclei (30, 71, 72). Unless the photoreactivity of DNA varies greatly from one nuclear region to another, the extent of damage is likely to be fairly con-

stant in all nuclear zones, and so any localization of repair must reflect differential accessibility to repair enzymes. Conversely, it is not possible to attribute the lethal effects of UV to absorption by particular zones, as has been done for ionizing radiation (36).

Though the cycle dependence of dimer formation may be due purely to changes in the target geometry, the cycle dependence of UV killing is only partly explicable by changes in dimer yield. Even after the D_qs have been converted from UV dose given to dimer formation, they are still substantially greater in mitosis and G_2 than in G_1 or S (Fig. 3*a*), and the D_0 in terms of dimers is greatest at the G_1/S boundary (Fig. 3*b*). If survival curves are to be interpreted for eukaryote cells as for bacteria—which may not be correct (73)—the changes in dimer D_q would indicate that cells irradiated in mitosis or G_2 have a greater capacity to repair dimer damage before it becomes lethal than do cells irradiated closer to or in S phase, and the changes in dimer D_0 would indicate that cells at the G_1/S boundary are best able to tolerate unrepaired dimers.

But though dimers are the best characterized lesion and are of proven biological importance (74), other photochemical lesions are becoming better understood, such as cytosine hydrates and DNA-protein cross-links; the latter, at least, show cycle-related formation (75). The coincidence reported here between the cycle dependence of dimer yield, changes in DNA sedimentation, and computed UV absorption by DNA does not necessarily lead to the conclusion that dimer formation, or even UV absorption by DNA, is the main lethal event. It is entirely possible that other lethal DNA photoproducts are formed together with dimers; and if so, the cycle-dependent variation in apparent dimer lethality may reflect changes in the ratio of formation of dimers to formation of other photoproducts, as well as in repair capacity. It is also possible that the lethal event involves UV absorption by DNA-associated chromatin proteins; since the shielding from UV of such molecules would be affected by the same factors as the shielding of the DNA they were bound to, their specific absorption would vary with the cycle in parallel with that of the DNA. But since the ratio of total chromatin protein to DNA is, in HeLa, at a minimum in mitosis and maximum in S phase (76), and the overall protein cross-linking is also at a maximum in S (75), the cycle-dependent variation in apparent dimer lethality which requires the hypothetical nondimer lethal lesion to be formed at a minimal rate, relative to dimers, in late S and at a maximum in mitosis would imply that lethal absorption and cross-linking by proteins are due to a subset of chromatin proteins whose abundance, or photoreactivity, varies inversely with that of the major proteins of the chromosomes. The simplest hypothesis, however, remains that cell killing is predominantly due to dimer formation.

We are grateful to Dr. S.L. Schor and Dr. A.M. Mullinger for their contributions to this work, and to Mr. R.G.W. Northfield and Mrs. E.G. Wilkin for their skilled assistance.

The investigation was supported by the Cancer Research Campaign and the Medical Research Council. R.T.J. is a Cancer Research Campaign Fellow.

Received for publication 28 January 1978 and in revised form 9 August 1978.

REFERENCES

1. RAO, P. N. 1968. Mitotic synchrony in mammalian cells treated with nitrous oxide at high pressure. *Science (Wash. D.C.).* **160**:774–776.
2. COLLINS, A. R. S., S. L. SCHOR, and R. T. JOHNSON. 1977. The inhibition of repair in UV irradiated human cells. *Mutat. Res.* **42**:413–432.

3. DULBECCO, R., and M. VOGT. 1954. Plaque formation and isolation of pure lines with poliomyelitis virus. *J. Exp. Med.* **99**:167–199.
4. WRAY, W. 1973. Isolation of metaphase chromosomes, mitotic apparatus and nuclei. *Methods Cell Biol.* **6**:283–306.
5. SEKIGUCHI, M., S. YASUDA, S. OKUBO, H. NAKAYAMA, K. SHIMADA, and Y. TAKAGI. 1970. Mechanism of repair of DNA in bacteriophage. I. Excision of pyrimidine dimers from ultraviolet-irradiated DNA by an extract of T4-infected cells. *J. Mol. Biol.* **47**:231–242.
6. FRICKE, U. 1975. Tritosol: a new scintillation cocktail based on Triton X-100. *Anal. Biochem.* **63**:555–558.
7. LATIMER, P., and C. A. H. EUBANKS. 1962. Absorption spectrophotometry of turbid suspensions: a method of correcting for large systematic distortions. *Arch. Biochem. Biophys.* **98**:274–285.
8. BURTON, K. 1956. A study of the conditions and mechanism of the diphenylamine reaction for the colorimetric estimation of deoxyribose nucleic acid. *Biochem. J.* **62**:315–323.
9. FRANKE, W. W., B. DEUMLING, H. ZENTGRAF, H. FALK, and P. M. M. RAE. 1973. Nuclear membranes from mammalian liver. IV. Characterization of membrane-attached DNA. *Exp. Cell Res.* **38**:272–284.
10. LINDSTRÖM, M., A. ZETTERBERG, and L. CARLSON. 1966. Quantitative microspectrophotometric analysis of nucleic acids in concentrated solutions, in solid droplets and in lymphocytes. *Exp. Cell Res.* **43**:537–545.
11. MELLORS, R. C., R. E. BERGER, and H. G. STREIM. 1950. Ultraviolet microscopy and microspectroscopy of resting and dividing cells. *Science (Wash. D.C.).* **111**:627–632.
12. DAVIES, H. G. 1954. The action of fixatives on the ultra-violet-absorbing components of chick fibroblasts. *Q. J. Microsc. Sci.* **95**:433–457.
13. CHU, E. H. Y. 1965. Effects of ultraviolet radiation on mammalian cells: I. Induction of chromosome aberrations. *Mutat. Res.* **2**:75–94.
14. BRUNSTING, A., and P. F. MULLANEY. 1972. Light scattering from coated spheres: model for biological cells. *Appl. Opt.* **11**:675–680.
15. OSTER, G. 1954. Light scattering. *Phys. Tech. Biol. Res.* **1**:51–73.
16. CASPERSSON, T. 1950. Cell Growth and Cell Function. W.W. Norton & Co. Inc., New York. 28–30.
17. MEYER, R. A., and A. BRUNSTING. 1975. Light scattering from nucleated biological cells. *Biophys. J.* **15**:191–203.
18. KILLANDER, D., and A. ZETTERBERG. 1965. Quantitative cytochemical studies on interphase growth. *Exp. Cell Res.* **38**:272–284.
19. ZETTERBERG, A. 1966. Nuclear and cytoplasmic nucleic acid content and cytoplasmic protein synthesis during interphase in mouse fibroblasts *in vitro*. *Exp. Cell Res.* **43**:517–525.
20. COMINGS, D. E., and T. A. OKADA. 1973. DNA replication and the nuclear membrane. *J. Mol. Biol.* **75**:609–618.
21. STUBBLEFIELD, E., and G. C. MUELLER. 1962. Molecular events in the reproduction of animal cells. II. The focalised synthesis of DNA in the chromosomes of HeLa cells. *Cancer Res.* **22**:1091–1099.
22. KAPP, L. N., and R. B. PAINTER. 1977. Multiple thymidine incorporation peaks in the S phase of synchronised human diploid fibroblasts. *Exp. Cell Res.* **107**:429–431.
23. DEWEY, W. C., J. S. NOEL, and C. M. DETTOR. 1972. Changes in radiosensitivity and dispersion of chromatin during the cell cycle of synchronous Chinese hamster cells. *Radiat. Res.* **52**:373–394.
24. DU PRAW, E. J. 1972. Quantitative constraints in the arrangement of human DNA. *Cold Spring Harbor Symp. Quant. Biol.* **38**:87–98.
25. CLEAVER, J. E. 1974. Sedimentation of DNA from human fibroblasts irradiated with ultraviolet light: possible detection of excision breaks in normal and repair-deficient xeroderma pigmentosum cells. *Radiat. Res.* **57**:207–227.
26. JOLLEY, G. M., and M. G. ORMEROD. 1974. The incomplete separation of complementary strands of high molecular weight DNA in alkali. *Biochim. Biophys. Acta.* **353**:200–214.
27. LINN, J. D., and K. T. WHEELER. 1975. Alkali unwinding kinetics of mammalian DNA in a simulated viscoelastometry experiment. *Biochem. Biophys. Res. Commun.* **66**:712–716.
28. RYDBERG, B. 1975. The rate of strand separation in alkali of DNA of irradiated mammalian cells. *Radiat. Res.* **61**:274–287.
29. BURG, K., A. R. S. COLLINS, and R. T. JOHNSON. 1977. Effects of ultraviolet light on synchronized Chinese hamster ovary cells: potentiation by hydroxyurea. *J. Cell Sci.* **28**:29–48.
30. JOHNSON, R. T., and K. SPERLING. Pattern of ultraviolet light induced repair in metaphase and interphase chromosomes. *Int. J. Radiat. Biol.* In press.
31. OKUBO, S., H. NAKAYAMA, and Y. TAKAGI. 1971. Repair of ultraviolet-damaged DNA in *Micrococcus lysodeikticus*. II. *In vivo* investigation on endonuclease activity for ultraviolet-irradiated DNA. *Biochim. Biophys. Acta.* **228**:83–94.

32. BACCHETTI, S., A. VAN DER PLAS, and G. VELDHUISEN. 1972. A UV-specific endonucleolytic activity present in human cell extracts. *Biochem. Biophys. Res. Commun.* **48**:662–669.
33. DUKER, N. J., and G. W. TEEBOR. 1975. Different ultraviolet DNA endonuclease activity in human cells. *Nature (Lond.).* **255**:82–84.
34. DINGMAN, C. W., and T. KAKUNAGA. 1976. DNA strand breaking and rejoining in response to ultraviolet light in normal human and xeroderma pigmentosum cells. *Int. J. Radiat. Biol.* **30**:55–66.
35. JAGGER, J. 1967. Introduction to Research in Ultraviolet Photobiology. Prentice-Hall, Inc., Englewood Cliffs, N.J. 61–63.
36. ZERMONO, A., and A. COLE. 1969. Radiosensitive structure of metaphase and interphase hamster cells as studied by low-voltage electron beam irradiation. *Radiat. Res.* **39**:669–684.
37. ICHIHASHI, M., and C. A. RAMSAY. 1976. The action spectrum and dose response studies of unscheduled DNA synthesis in normal human fibroblasts. *Photochem. Photobiol.* **23**:103–106.
38. ALVAREZ, M. R. 1975. Microfluorometric comparisons of heat-induced nuclear acridine orange metachromasia between normal cells and neoplastic cells from primary tumors of diverse origin. *Cancer Res.* **35**:93–98.
39. PEDERSON, T. 1972. Chromatin structure and the cell cycle. *Proc. Natl. Acad. Sci. U.S.A.* **69**:2224–2228.
40. PEDERSON, T., and E. ROBBINS. 1972. Chromatin structure and the cell division cycle. Actinomycin binding in synchronised HeLa cells. *J. Cell. Biol.* **55**:322–327.
41. HILDEBRAND, C. E., and R. A. TOBEY. 1975. Cell-cycle specific changes in chromatin organisation. *Biochem. Biophys. Res. Commun.* **63**:134–139.
42. SCHOR, S. L., R. T. JOHNSON, and C. A. WALDREN. 1975. Changes in the organization of chromosomes during the cell cycle: Response to ultraviolet light. *J. Cell Sci.* **17**:539–565.
43. NICOLINI, C., K. AJIRO, T. W. BORUN, and R. BASERGA. 1975. Chromatin changes during the cell cycle of HeLa cells. *J. Biol. Chem.* **250**:3381–3385.
44. DARZYNKIEWICZ, Z., F. TRAGANOS, T. SHARPLESS, and N. R. MELAMED. 1977. Differential sensitivity of DNA *in situ* in interphase and metaphase chromatin to heat denaturation. *J. Cell Biol.* **73**:128–138.
45. SETLOW, R. B., and W. L. CARRIER. 1966. Pyrimidine dimers in ultraviolet-irradiated DNA. *J. Mol. Biol.* **17**: 237–254.
46. CHALMERS, A. H., M. LAVIN, S. ATISOONTORKUL, J. MANSBRIDGE, and C. KIDSON. 1976. Resistance of human melanoma cells to ultraviolet radiation. *Cancer Res.* **36**:1930–1934.
47. ISOMURA, K., O. NIKAIDO, M. HORIKAWA, and T. SUGAHARA. 1973. Repair of DNA damage in ultraviolet-sensitive cells isolated from HeLa S3 cells. *Radiat. Res.* **53**:143–152.
48. BUHL, S. N., R. M. STILLMAN, R. B. SETLOW, and J. D. REGAN. 1972. DNA chain elongation and joining in normal human and xeroderma pigmentosum cells after ultraviolet irradiation. *Biophys. J.* **12**:1183–1191.
49. RAUTH, A. M., M. TAMMEMAGI, and G. HUNTER. 1974. Nascent DNA synthesis in ultraviolet light-irradiated mouse, human, and Chinese hamster cells. *Biophys. J.* **14**:209–220.
50. WATANABE, M., and M. HORIKAWA. 1974. Analyses of differential sensitivities of synchronised HeLa S3 cells to radiations and chemical carcinogen during the cell cycle. II. Ultraviolet light. *Biochem. Biophys. Res. Commun.* **58**:185–191.
51. STEWARD, D. L., and R. M. HUMPHREY. 1966. Induction of thymine dimers in synchronised populations of Chinese hamster cells. *Nature (Lond.).* **212**:298–300.
52. TROSKO, J. E., M. KASSCHAU, L. COVINGTON, and E. H. Y. CHU. 1966. UV induction of pyrimidine dimers during different phases of the cell cycle of mammalian cells. *Radiat. Res.* **27**:535.
53. ERIKSON, R. L., and W. SZYBALSKI. 1963. Molecular radiobiology of mammalian cell lines. IV. Variation in ultraviolet light and X-ray sensitivity during the division cycle. *Radiat. Res.* **18**:200–212.
54. TODD, P., H. DALEN, and C. B. SCHROY. 1977. Survival of synchronous cultured human liver cells following single and fractionated exposures to ultraviolet light. *Radiat. Res.* **69**:573–582.
55. SINCLAIR, W. A., and R. A. MORTON. 1965. X ray and ultraviolet sensitivity of synchronised Chinese hamster cells at various stages of the cell cycle. *Biophys. J.* **5**:1–25.
56. RAUTH, A. M., and G. F. WHITMORE. 1966. The survival of synchronised L cells after ultraviolet irradiation. *Radiat. Res.* **28**:84–95.
57. DJORDJEVIC, B., and L. J. TOLMACH. 1967. Responses of synchronous populations of HeLa cells to ultraviolet light at selected stages of the generation cycle. *Radiat. Res.* **32**:327–346.
58. HAN, A., and W. K. SINCLAIR. 1969. Sensitivity of synchronised Chinese hamster cells to ultraviolet light. *Biophys. J.* **9**:1171–1192.
59. WATANABE, W., and M. HORIKAWA. 1973. Analyses of differential sensitivities of synchronized HeLa S3 cells to radiations and chemical carcinogen during the cell cycle. *J. Radiat. Res.* **14**:258–270.
60. MARMUR, J., W. F. ANDERSON, L. MATTHEWS, K. BERNS, E. GAJEWSKA, D. LANE, and P. DOTY. 1961. The

effects of ultraviolet light on the biological and physical chemical properties of deoxyribonucleic acids. *J. Cell. Comp. Physiol.* **58**(Suppl. 1):33–55.

61. SALGANIK, R. I., V. F. DREVICH, and E. A. VASYUNINA. 1967. Isolation of ultraviolet-denatured regions of DNA and their base composition. *J. Mol. Biol.* **30**:219–222.
62. HAYES, F. N., D. LL. WILLIAMS, R. L. RATLIFF, A. J. VARGHESE, and C. S. RUPERT. 1971. Effect of a single thymine photodimer on the oligodeoxythymidylate-polydeoxyadenylate interactions. *J. Am. Chem. Soc.* **93**:4940–4942.
63. LANG, H., and G. LUCK. 1973. Ultraviolet-light-induced conformational changes in DNA. *Photochem. Photobiol.* **17**:387–393.
64. GUPTA, R. D., and S. MITRA. 1974. Strand separation of DNA induced by ultraviolet irradiation *in vitro*. *Biochim. Biophys. Acta.* **374**:145–158.
65. WEINBLUM, D., H. J. BRETER, R. K. ZAHN, and J. BERGER. 1974. Alteration of DNA reassociation kinetics due to base mismatch caused by thymine dimerisation. *Biochim. Biophys. Acta.* **374**:324–331.
66. STAFFORD, R. S., D. P. ALLISON, and R. O. RAHN. 1975. Detection by electron microscopy of photo-induced denaturation in λ DNA. *Nucleic Acid Res.* **2**:143–148.
67. BRENT, T. P. 1972. Repair enzyme suggested by mammalian endonuclease activity specific for ultraviolet-irradiated DNA. *Nat. New Biol.* **239**:172–173.
68. BURR, J. G. 1968. Advances in the photochemistry of nucleic acid derivatives. *Adv. Photochem.* **6**:193–299.
69. COLLINS, J. M. 1977. Deoxyribonucleic acid structure in human diploid fibroblasts stimulated to proliferate. *J. Biol. Chem.* **252**:141–147.
70. HSU, T. C. 1975. A possible function of constitutive heterochromatin: the bodyguard hypothesis. *Genetics.* **79** (Suppl.):137–150.
71. HARRIS, C., R. J. CONNOR, F. E. JACKSON, and M. W. LIEBERMAN. 1974. Intranuclear distribution of DNA repair synthesis induced by chemical carcinogens or ultraviolet light in human diploid fibroblasts. *Cancer Res.* **34**:3461–3468.
72. BERLINER, J., S. W. HIMES, C. T. AOKI, and A. NORMAN. 1975. The sites of unscheduled DNA synthesis within irradiated human lymphocytes. *Radiat. Res.* **63**:544–552.
73. WILLIAMS, J. R., and J. B. LITTLE. 1977. Selective protection of cultured human cells from the toxic effect of ultraviolet light by proflavin treatment. *Radiat. Res.* **72**:154–163.
74. GRIGGS, H. G., and M. A. BENDER. 1972. Ultraviolet and gamma-ray induced reproductive death and photoreactivation in a *Xenopus* tissue culture cell line. *Photochem. Photobiol.* **15**:517–526.
75. HAN, A. M., M. KORBELICK, and J. BAN. 1975. DNA-to-protein crosslinking in synchronous HeLa cells exposed to ultraviolet light. *Int. J. Radiat. Biol.* **27**:63–74.
76. KARN, J., E. M. JOHNSON, G. VIDALI, and V. G. ALLFREY. 1974. Differential phosphorylation and turnover of nuclear acidic proteins during the cell cycle of HeLa Cells. *J. Biol. Chem.* **249**:667–677.
77. WHEELER, K. T., J. DEWITT, and J. T. LETT. 1974. A marker for mammalian DNA sedimentation. *Radiat. Res.* **57**:365–378.